

Excited states dynamics in time-dependent density functional theory: high-field molecular dissociation and harmonic generation.

Alberto Castro^{1,2,3}, M. A. L. Marques², Julio A. Alonso¹, George F. Bertsch³ and Angel Rubio²

¹*Departamento de Física Teórica, Universidad de Valladolid, 47011 Valladolid (Spain)*

²*Departamento de Física de Materiales, Facultad de Químicas, Universidad del País Vasco; Centro Mixto CSIC-UPV/EHU and Donostia International Physics Centre (DIPC), 20080 San Sebastián (Spain)*

³*Physics Department and Institute for Nuclear Theory, University of Washington, Seattle WA 98195 (USA)*

We present a theoretical description of femtosecond laser induced dynamics of the hydrogen molecule and of singly ionised sodium dimers, based on a real-space, real-time, implementation of time-dependent density functional theory (TDDFT). High harmonic generation, Coulomb explosion and laser induced photo-dissociation are observed. The scheme also describes non-adiabatic effects, such as the appearance of even harmonics for homopolar but isotopically asymmetric dimers, even if the ions were treated classically. This TDDFT-based method is reliable, scalable, and extensible to other phenomena such as photoisomerization, molecular transport and chemical reactivity.

PACS numbers: 33.80.Gj, 33.80.Wz, 42.50.Hz

It is now possible to study electron and molecular dynamics in real time using various experimental techniques employing intense ultra-short laser sources [1]. Some examples of such investigations include X-ray photoelectron spectroscopy of molecules [2], pump-probe ionisation measurements [3], production of high harmonics as a source of soft X-rays [4], the measurement of electron-phonon interactions in thin films [5], and the estimation of the onset of Coulomb screening [6]. A technologically important and very active field of research is the application of ultra-short laser pulses to induce, control and monitor chemical reactions [7, 8, 9]. Whenever the intensity of the laser field is comparable to the molecular electronic fields, perturbative expansions break down and new processes appear, which are not fully understood from a microscopical point of view [10]. A practical and accurate computational framework to describe excited-state electron-ion dynamics is therefore still needed.

Not surprisingly, the smallest systems have attracted particular attention from both experimentalists and theoreticians, as a bench-horse to improve our understanding of electron dynamics at the femtosecond scale [11, 12]. However, the methods used in these calculations can not be easily extended to larger and more realistic systems. The exact quantum mechanical solution of a 3D system of more than three particles is certainly not feasible with state-of-the-art computers. 1D models are much easier to handle, but they can not really be used as predictive tools for problems involving the interaction of lasers with large clusters or solid-state systems of technological relevance.

To tackle such a problem, time-dependent density functional theory (TDDFT) [18] appears as a valuable tool. Even with the simplest approximation to the exchange-correlation potential, the adiabatic local density approximation (ALDA), one obtains a very good compromise between computational ease and accuracy [19]. TDDFT can certainly be applied to large systems in non perturbative regimes, while providing a consistent treatment of electron correlation. It has been well tested

in the study of electron excitations, like the optical absorption spectra in the linear regime [20, 21]. Although almost all applications of TDDFT in the field of laser physics have only involved electronic dynamics, recent attempts have also been made at describing the coupled nuclear and electronic motion in laser fields [22], accounting for the nuclear motion classically. A full quantum mechanical treatment of the system could in principle be done within a multi-component TDDFT, although it has not been tried for more than three particles [23]. However, since many vibrational quanta are coherently excited, there is good motivation for the classical treatment of the nuclei. The purpose of this work is to illustrate a general method to study many-electron systems subject to strong laser fields. It is based on the quantum mechanical propagation of the electronic wave packet – described within TDDFT – combined with classical motion of the nuclei. As the laser field populates the excited Born-Oppenheimer surfaces, this scheme includes diabatic effects, while maintaining a good scaling with the size of the system. As an illustration we focused on one and two electron dimers, namely Na_2^+ and the hydrogen molecule.

The equations of motion may be derived from the Lagrangian:

$$\mathcal{L} = \sum_{\alpha} \left[\frac{1}{2} m_{\alpha} \dot{\vec{R}}_{\alpha}^2 + Z_{\alpha} \vec{R}_{\alpha} \cdot \vec{\mathcal{E}}(t) \right] - \sum_{\alpha < \alpha'} \frac{Z_{\alpha} Z_{\alpha'}}{|\vec{R}_{\alpha} - \vec{R}_{\alpha'}|} \\ \sum_i \langle \phi_i | i \hbar \frac{\partial}{\partial t} - e \vec{x} \cdot \vec{\mathcal{E}}(t) | \phi_i \rangle - E_{DFT}(\{\phi\}, \{\vec{R}\}), \quad (1)$$

where E_{DFT} is the usual Kohn-Sham density functional, depending on the electron orbitals $\{\phi\}$ and the nuclear coordinates $\{\vec{R}\}$, and $\vec{\mathcal{E}}(t)$ is the time-dependent electric field from the laser pulse. Variation of the Lagrangian then yields Newton's equations for the nuclear coordinates,

$$m_{\alpha} \frac{d^2 \vec{R}_{\alpha}}{dt^2} = -\vec{\nabla}_{\vec{R}_{\alpha}} E_{DFT}$$

$$-\sum_{\alpha'} \frac{(\vec{R}_\alpha - \vec{R}_{\alpha'}) Z_\alpha Z_{\alpha'}}{|\vec{R}_\alpha - \vec{R}_{\alpha'}|^3} + Z_\alpha \vec{\mathcal{E}}(t), \quad (2)$$

and the usual TDDFT equations for the orbital variables [18]. We solved these equations in real time, following the method of Yabana and Bertsch [20], using a real-space grid representation of the orbitals [24, 25]. This scheme has the advantage that the Kohn-Sham Hamiltonian is a very sparse matrix. The forces in Eq. (2) are calculated with the help of a generalised Hellmann-Feynman theorem,

$$-\vec{\nabla}_{\vec{R}_\alpha} E_{DFT} = -\sum_i \langle \phi_i | \vec{\nabla}_\alpha H_{KS} | \phi_i \rangle. \quad (3)$$

where $H_{KS} = \delta E_{DFT} / \delta n(\mathbf{r}, t)$ is the Kohn-Sham Hamiltonian. For numerical reasons we represent the electron-ion interaction by norm-conserving non-local Troullier-Martins pseudopotentials [26].

We have studied two different classes of time-dependent problems: photofragmentation and high harmonic generation. We now discuss the first case, the Na_2^+ dimer in a femtosecond laser field. It is a good test, since it has been exhaustively studied using a diverseness of approaches [8, 14, 27]. In particular, a recent experiment [8] focused on the photofragmentation of Na_2^+ in intense femtosecond laser fields. Using a pump-probe technique, the authors discovered that Na_2^+ dissociated in four different channels, ranging from simple field ionisation followed by Coulomb explosion, to photodissociation on light-induced potentials. For these calculations, we used a uniform grid spacing of 0.3 Å, and the system was confined to a sphere of radius 10 Å. In these one-electron calculations, we omitted the core-valence exchange-correlation. In this case the total electronic energy is given by the Kohn-Sham eigenvalues, and they can be used to compute the adiabatic potential energy surfaces shown in Fig. 1. The two lowest single-photon transitions from the $1^2\Sigma_g^+$ ground state are at 2.5 eV (to the $1^2\Sigma_u^+$ state) and at 3.2 eV (to the $1^2\Pi_u$ state). The latter is achieved by a laser polarized perpendicularly to the internuclear axis. These energies accord well with the observed single-photon transitions [28]. For the time-dependent calculations, we start with the dimer in its ground state, which is then propagated with a modified Krank-Nicholson scheme [24]. The time step for the time integration was $0.005 \hbar \text{ eV}^{-1} \approx 0.003 \text{ fs}$. A simple check on the implementation of the time evolution operator consists of calculating the linear photo-absorption spectrum, using a weak δ -function external field, as in Ref. [20]. Almost all the spectral weight is concentrated in two peaks (see inset in Fig. 1), which are at energies corresponding exactly to the vertical transitions between energy surfaces. We note that this exact correspondance is only obtained for one-electron systems: in general the TDDFT spectra will have shifts from the energy surfaces determined by the Kohn-Sham eigenvalues.

Next we examine the evolution of the dimer under high-field excitation. We consider external fields of the

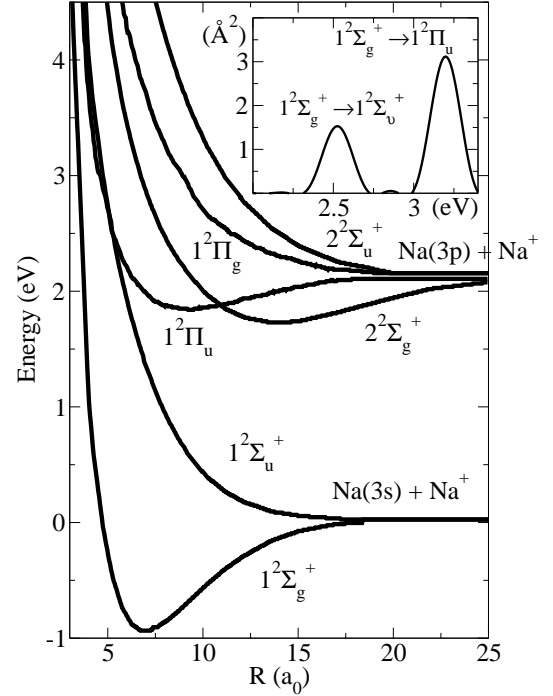


FIG. 1: Adiabatic energy surfaces of the Na_2^+ dimer, as obtained by our three-dimensional real-space code. Similar results can be found in Ref. [29]. In the inset, the computed photoabsorption cross-section of the same molecule.

form:

$$\vec{\mathcal{E}}(t) = \left(\frac{8\pi}{c} I_0 \right)^{(1/2)} \sin \left(\pi \frac{t}{\tau} \right) \sin(\omega t) \hat{e}, \quad 0 < t < \tau, \quad (4)$$

where I_0 is the maximum intensity of the pulse, \hat{e} is the polarization vector, and τ is the pulse duration, taken as $\tau = 80 \text{ fs}$. As a first case, we examine the effect of excitation at the lower resonant frequency, $\omega = 2.5 \text{ eV}$. In Fig. 2(a), we present a series of runs at different intensities, ranging from weak (10^{10} W/cm^2) to moderate ($2.1 \times 10^{12} \text{ W/cm}^2$). Since the $1^2\Sigma_u^+$ surface is anti-bonding, excitation at this resonant frequency should lead to dissociation, even at moderate intensities. This is indeed confirmed by our calculations. The upper panel depicts the internuclear separation of the dimer, which exhibits an acceleration during the laser pulse and a nearly constant velocity expansion thereafter. Clearly, the dimer dissociates at all field levels that we applied. To examine the ionisation of the dimer, we assumed that any density reaching the edges of the simulation box corresponds to unbound electrons. By absorbing this density at the boundaries, we can thus define the ionisation probability as $I(t) = 1 - N(t)$, where $N(t)$ is the charge that remains inside the simulation box at time t . The lower panel of Fig. 2(a) shows N as a function of t . We see that there is practically no ionisation for the lower fields, and only a 20% ionization probability for the $2.1 \times 10^{12} \text{ W/cm}^2$ field.

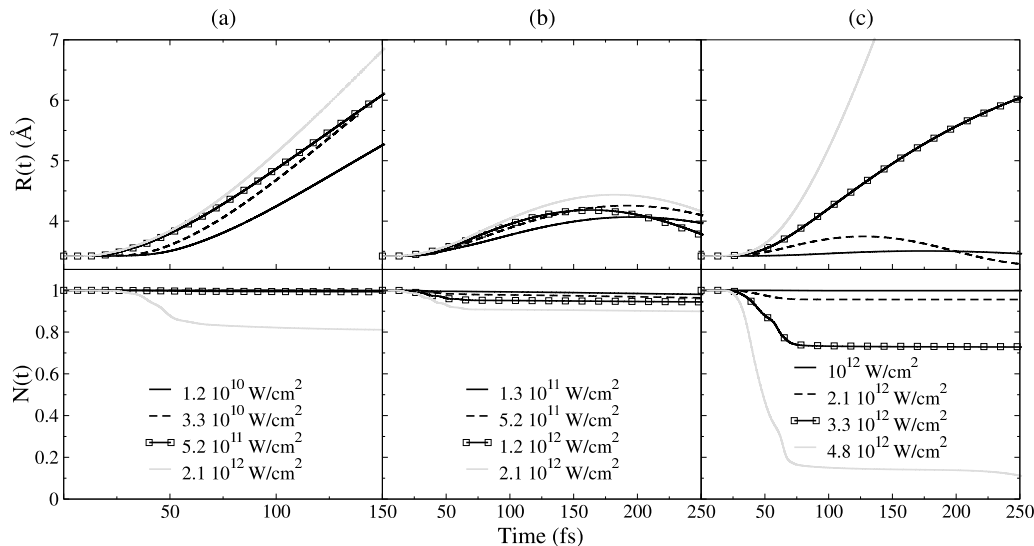


FIG. 2: Evolution of internuclear distance (top panel) and electronic charge in simulation region (bottom panel) for the Na_2^+ molecule. The dimers are excited with laser pulses of 2.5, 3.2 and 1.57 eV in columns (a), (b) and (c) respectively.

Thus, in this range of intensities, the laser dissociates the dimer without ionising it.

We next consider the excitation at the upper resonance frequency, $\omega = 3.2 \text{ eV}$, corresponding to an electric field perpendicular to the dimer axis. Since the $1^2\Pi_u$ surface is bonding, [see Fig. 2 (b)] no dissociation is expected unless the Coulomb explosion channel is opened through ionisation. We see that the dimer remains bound over the entire range of intensities that produced dissociation at the lower resonant frequency.

Finally, we also performed simulations at the non-resonant frequency $\omega = 1.57 \text{ eV}$, the one used in Ref.

[8]. Fig. 2 (c) shows how dissociation now occurs only at much higher intensities, and it is mainly due to ionisation (almost absent in the resonant calculations for the range of intensities used): since Na_2^+ has no bonding states, ionisation is followed by Coulomb explosion.

Another process in which the nuclear motion may play an important role is high harmonic generation. Even harmonics may be created by irradiating HD with an intense laser pulse, but not by irradiating H_2 : even harmonic generation is forbidden for a centrosymmetric molecule. In an adiabatic treatment of the nuclear coordinates, the nuclear masses play no role and the even harmonics can not appear. This is no longer the case if non-adiabatic effects are taken into account, for the different masses of H and D break the symmetry. Kreibich et al. [17] studied this process in a 1-D model with a full quantum mechanical treatment of the nuclear motion, finding strong even harmonics at high harmonic number. To discern whether the classical treatment of nuclear motion also produces these harmonics, we studied the same 1D problem within our framework. As in Ref. [17], we took the laser field to have a frequency of 1.6 eV, and an intensity that rises linearly to 10^{14} W/cm^2 over an interval of 10 optical cycles, and is held constant thereafter. We then calculated the spectral intensity of the generated harmonics, $H(\omega)$:

$$H(\omega) \sim \left| \int dt e^{i\omega t} \frac{d^2}{dt^2} \langle \Psi(t) | \hat{e} \cdot \vec{D} | \Psi(t) \rangle \right|^2. \quad (5)$$

We find that the classical treatment does indeed produce even harmonics, but much smaller than the quantum treatment. The results are shown in Fig. 3. The top left panel depicts the harmonic spectrum for HD, and only odd harmonics are apparent. However, it may be proved that the HD Hamiltonian already violates centrosymmetry within our classical treatment, through a

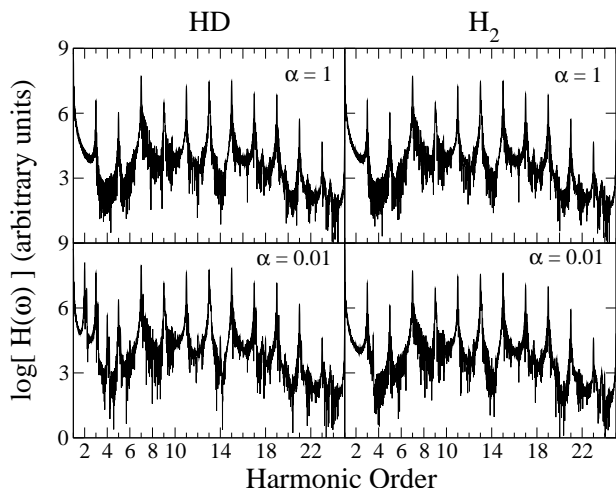


FIG. 3: Harmonic spectra of HD (left panels) and H_2 (right panels). The nuclear masses used in the calculation are $m' = \alpha m$, being m the real mass. In this way, top plots were made using for the nuclear masses their real values whereas bottom plots were made using a hundredth of their real values.

term of the form:

$$-\frac{1}{2} \left(\frac{1}{M_H} - \frac{1}{M_D} \right) P(t) (\hat{p}_1 + \hat{p}_2),$$

where $P(t) = \frac{1}{2}(P_H(t) - P_D(t))$ is the relative time-dependent nuclear momentum and \hat{p}_i are the electronic momentum operators [30]. Its effect can be enhanced by decreasing the nuclear masses. In the bottom left panel, the H and D masses have been decreased by a factor 100, and then the second- and fourth-order harmonics become visible. As a qualitative check of the numerics, we also show the same graphs for H_2 , in which no even harmonics can occur.

Thus we see that on qualitative level the non-adiabatic dynamics generating even harmonics are obtained with the classical treatment of the nuclear coordinates. However, the quantum treatment may be needed for a quantitative result. By describing the nuclei quantum mechanically, the ground state violates centrosymmetry and the even harmonics can be generated even if the nuclear motion is frozen. In contrast, in the classical treatment the ground state is symmetric and the symmetry violation only builds up as the nuclei move.

In summary, we have examined the computational feasibility of including nuclear dynamics in time-dependent

density functional theory using a pseudopotential code to study the femtosecond laser induced dynamics of sodium dimers. Using this approach for treating the Na_2^+ dimer, we were able to distinguish different photodissociation regimes, ranging from dissociation on light induced potentials, to field ionisation followed by Coulomb explosion. Electronic and ionic degrees of freedom are thus coupled, so that one can observe the electron-phonon transfer of energy. We also found, with another example, that non-adiabatic effects are present in the general treatment based on Eq. (1). One of the major attractiveness of this method resides in its reasonable scaling behaviour when applied to larger systems. We thus expect to be able to tackle problems like photoisomerization or even photochemical reactivity in systems of dozens of atoms in the near future.

This work was supported by the RTN program of the European Union NANOPHASE (contract HPRN-CT-2000-00167), Basque Country University, Iberdrola S.A. and DGESIC (PB98-0345). GB acknowledges support by the US Department of Energy under Contract Nr. E-FG-06-90ER-411132. Computer time was kindly provided by the CEPBA. We thank E. K. U. Gross for enlightenment discussions. AC thanks the University of Washington and the DIPC for kind hospitality.

-
- [1] For a review, see T. Brabec and F. Krausz, Rev. Mod. Phys. **72**, 545 (2000). For recent developments, see M. Drescher *et al.*, Science **291**, 1923 (2001) and M. Hentschel *et al.*, Nature **414**, 509 (2001).
 - [2] L. N.-Glandorf *et al.*, Phys. Rev. A **62**, 023812 (2000); Phys. Rev. Lett. **87**, 193002 (2001).
 - [3] See, for example, articles in Faraday Discussions **115** (2000).
 - [4] Z. Chang *et al.*, Phys. Rev. Lett. **79**, 2967 (1997); C. Spiedelmann *et al.*, Science **278**, 671 (1997).
 - [5] M. Probst and R. Haight, Appl. Phys. Lett. **71**, 202 (1997).
 - [6] R. Huber *et al.*, Nature **414**, 286 (2001).
 - [7] C. Dion *et al.*, J. Chem. Phys. **105**, 9083 (1996); R. W. Shoenlein *et al.*, Science **254**, 412 (1991).
 - [8] A. Assion, T. Baumert, U. Weichmann, and G. Gerber, Phys. Rev. Lett. **86**, 5695 (2001).
 - [9] K. Yamanouchi, Science **295**, 1659 (2002).
 - [10] Examples commonly invoked are bond softening, vibrational population trapping, molecular alignment and above threshold dissociation.
 - [11] M. Protopapas, C. H. Keitel, and P. L. Knight, Rep. Prog. Phys. **60**, 389 (1997).
 - [12] Some of the works include exact 3D calculations for one and two electron atoms [13], for one electron dimers [14], and 1D models for two electron systems [15, 16, 17].
 - [13] J. Parker *et al.*, J. Phys. B **29**, L33 (1996).
 - [14] S. Magnier, M. Persico, and N. Rahman, J. Phys. Chem. A **103**, 10691 (1999).
 - [15] R. Grobe and J. H. Eberly, Phys. Rev. A **48**, 4664 (1993); D. G. Lappas *et al.*, J. Phys. B **29**, L619 (1996).
 - [16] M. Lein, E. K. U. Gross, and V. Engel, Phys. Rev. A **64**, 023406 (2001).
 - [17] T. Kriebich *et al.*, Phys. Rev. Lett. **87**, 103901 (2001).
 - [18] E. Runge and E. K. U. Gross, Phys. Rev. Lett. **52**, 997 (1984); E. K. U. Gross, J. F. Dobson, and M. Petersilka, in *Density Functional Theory II*, edited by R.F. Nalewajski, "Topics in Current Chemistry", Vol 181 (Springer, Berlin, 1996).
 - [19] The ALDA has nevertheless some well known problems, but most of them can be solved by the swarm of exchange-correlation potential now available – see, for example, M. A. L. Marques, A. Castro, and A. Rubio, J. Chem. Phys. **115**, 3006 (2001), and references therein.
 - [20] K. Yabana and G. F. Bertsch, Phys. Rev. B **54**, 4484 (1996); Int. J. Quantum Chem. **75**, 55 (1999).
 - [21] G. Onida, L. Reining, and A. Rubio, Rev. Mod. Phys. (2002) and references therein.
 - [22] F. Calvayrac *et al.*, Phys. Rep. **337**, 493 (2000); E. Suraud and P. G. Reinhard, Phys. Rev. Lett. **85**, 2296 (2000).
 - [23] T. Kriebich and E. K. U. Gross, Phys. Rev. Lett. **86**, 2984 (2001).
 - [24] H. Flocard, S. E. Koonin, and M. S. Weiss, Phys. Rev. C **17**, 1682 (1978).
 - [25] J. R. Chelikowsky, N. Trouiller, and Y. Saad, Phys. Rev. Lett. **72**, 1240 (1994); A. Rubio *et al.*, Phys. Rev. Lett. **77**, 247 (1996); T. L. Beck, Rev. Mod. Phys. **72**, 1041 (2000).
 - [26] N. Troullier and J. L. Martins, Phys. Rev. B **43**, 1993 (1991).
 - [27] S. Magnier, M. Persico, and N. Rahman,

- Chem. Phys. Lett. **262**, 747 (1996); M. Machholm and A. Suzor-Weiner, J. Chem. Phys. **105**, 971 (1996).
- [28] V. Bonačić-Koutecký *et al.*, J. Chem. Phys. **104**, 1427 (1996).
- [29] S. Magnier, F. Oise, and M. Seeuws, Mol. Phys. **89**, 711 (1996).
- [30] A canonical transformation to the nuclear geometrical center has been performed.